Draft version November 6, 2012
Preprint typeset using LaTeX style emulateapj v. 5/2/11

PROSPECTS FOR MEASURING THE RELATIVE VELOCITIES OF GALAXY CLUSTERS IN PHOTOMETRIC SURVEYS USING THE KINETIC SUNYAEV-ZEL'DOVICH EFFECT

Ryan Keisler[1,2,3], Fabian Schmidt[4,5]

Draft version November 6, 2012

ABSTRACT

We consider the prospects for measuring the pairwise kinetic Sunyaev-Zel'dovich (kSZ) signal from galaxy clusters discovered in large photometric surveys such as the Dark Energy Survey (DES). We project that the DES cluster sample will, in conjunction with existing mm-wave data from the South Pole Telescope (SPT), yield a detection of the pairwise kSZ signal at the 8-13σ level, with sensitivity peaking for clusters separated by $\sim$100 Mpc distances. A next-generation version of SPT would allow for a 18-30σ detection and would be limited by variance from the kSZ signal itself and residual thermal Sunyaev-Zel'dovich (tSZ) signal. Throughout our analysis we assume photometric redshift errors, which wash out the signal for clusters separated by $\lesssim$50 Mpc; a spectroscopic survey of the DES sample would recover this signal and allow for a 26-43σ detection, and would again be limited by kSZ/tSZ variance. Assuming a standard model of structure formation, these high-precision measurements of the pairwise kSZ signal will yield detailed information on the gas content of the galaxy clusters. Alternatively, if the gas can be sufficiently characterized by other means (*e.g.* using tSZ, X-ray, or weak lensing), then the relative velocities of the galaxy clusters can be isolated, thereby providing a precision measurement of gravity on 100 Mpc scales. We briefly consider the utility of these measurements for constraining theories of modified gravity.

1. INTRODUCTION

Measurements of the peculiar velocities of massive halos, in conjunction with expansion history measurements, can be used to constrain cosmological models and test gravity on cosmological scales (Kosowsky & Bhattacharya 2009; Reyes et al. 2010). The kinetic Sunyaev-Zel'dovich (kSZ) effect (Sunyaev & Zel'dovich 1972) effect provides a means to measure peculiar velocities. CMB photons gain or lose energy after Thomson scattering on free electrons moving with respect to the CMB, and the resulting shift in the CMB temperature in the direction of the electrons is known as the kSZ effect.

The kSZ effect was recently measured at the 3.8σ level (Hand et al. 2012) using mm-wave data from the Atacama Cosmology Telescope (ACT) in conjunction with the BOSS spectroscopic catalog (SDSS-III Collaboration et al. 2012). This was a measurement of the *pairwise* kSZ signal; two massive halos will tend to fall towards each other, and the resulting CMB temperature difference is the pairwise kSZ signal.

The cosmological utility of a catalog of kSZ-derived velocities was studied in detail in Bhattacharya & Kosowsky (2007) and Kosowsky & Bhattacharya (2009), and the prospects for measuring growth using the angular correlation of galaxies found in the Dark Energy Survey[6] (DES) was studied by Ross et al. (2011). In this letter we consider the prospects for detecting the pairwise kSZ signal using existing or future mm-wave data from the South Pole Telescope (SPT, Carlstrom et al. (2011)) and galaxy clusters discovered by the DES, which is coming online at the time of writing. We simulate photometric redshift errors and realistic mm-wave data, including the noise introduced by the tSZ and kSZ effects, and find that these datasets will yield strong detections of the pairwise kSZ signal.

rkeisler@uchicago.edu, fabians@astro.princeton.edu
[1] Kavli Institute for Cosmological Physics, University of Chicago, 5640 South Ellis Avenue, Chicago, IL 60637, USA
[2] Department of Physics, University of Chicago, 5640 South Ellis Avenue, Chicago, IL 60637, USA
[3] Hubble Fellow
[4] Department of Astrophysical Sciences, Princeton University, Princeton, NJ 08540, USA
[5] Einstein Fellow
[6] http://www.darkenergysurvey.org

2. ANALYSIS

Our analysis relies on the simulations presented in Sehgal et al. (2010), hereafter S10. This work constructed simulated maps of the mm-wave sky with contributions from the CMB, the thermal and kinetic SZ effects, and emissive sources. The pieces of S10 that are relevant for our analysis are the halo catalog and the simulated maps of the kSZ and tSZ signals. The SZ signals were calculated per cluster in post-processing; the gravitational potential was calculated according to the N-body particle density, and the gas density and pressure were calculated assuming hydrostatic equilibrium and a polytropic equation of state. S10 calculated the kSZ signal after assigning a single, mass-averaged velocity to all gas associated with each cluster. We scale the S10 tSZ map by a factor of 0.7, which is in broad agreement with the signals measured in recent tSZ cluster surveys (Benson et al. 2011) and measurements of the tSZ power spectrum (Reichardt et al. 2012).

2.1. *Cluster Sample*

We construct two DES-like cluster samples from the S10 halo catalog. The first, dubbed DES-*base*, includes clusters with $1 \times 10^{14}\ M_\odot < M_{500c} < 3 \times 10^{14}\ M_\odot$ and $0.2 < z < 1.0$. The lower mass threshold, $M_{500c} = 1 \times 10^{14}\ M_\odot$, corresponds to approximately 20 galaxies (Rykoff et al. 2012), which is the expected selection threshold for DES clusters. We ignore scatter in mass (at

fixed optical richness) and offsets between the optically-derived cluster center and the center of gas mass, both of which would need to be modeled in a more realistic analysis. The second, more aggressive sample, dubbed DES-*agg*, has the same redshift range but a lower mass range: $5 \times 10^{13}\ M_\odot < M_{500c} < 1.5 \times 10^{14}\ M_\odot$. Such low mass systems might be obtained in exchange for lower purity and higher mass scatter.

We have limited the upper mass range of these samples to create more uniform samples and to mitigate strong tSZ signals. This requirement reduces the number density of clusters by ∼10% per sample, leading to ∼4 (16) clusters per deg^2 in the DES-*base* (DES-*agg*) sample.

We assign photometric redshift errors to the cluster redshifts according to $\sigma_z = 0.01 \times \exp(z/2.5)$, approximating the DES photometric errors presented in *The Supplements for the Dark Energy Survey White Paper*[7]. The mean redshifts are the redshifts provided in the S10 catalog, which do not include distortions due to velocities

2.2. *mm-wave Data*

We simulate observations of the mm-wave sky by the SPT. We consider two surveys:

- SPT-SZ - the initial, 2500 deg^2 survey, for which we assume white noise levels of [40, 18, 80] μK-arcminute and beam widths of [1.6, 1.05, 0.85] arcminute FWHM at [95, 150, 220] GHz, and
- SPT-3G - a future, third-generation survey, which covers the same 2500 deg^2 area, and for which we assume white noise levels of [4.3, 2.5, 4.3] μK-arcminute and beam widths of [1.6, 1.05, 0.85] arcminute FWHM at [95, 150, 220] GHz.

While each of these surveys has or would have coverage at 95, 150, and 220 GHz, we use only the 150 and 220 GHz data in the simplified analysis presented here (with one exception, discussed in Section 2.5). We assume a background of randomly-distributed, emissive sources with $\sqrt{C_\ell} = 7$ (21.5) μK-arcminute at 150 (220) GHz that is perfectly spatially correlated between 150 and 220 GHz, consistent with the results of Reichardt et al. (2012). We optimally combine the 150 and 220 GHz data as a function of multipole to minimize the total power due to instrumental noise and emissive sources, and the resulting noise power is defined as N_ℓ. The beam-deconvolved noise power at $\ell = 4000$, where the kSZ sensitivity peaks, is $\sqrt{N_{4000}}$ ∼22 μK-arcminute (6 μK-arcminute) for SPT-SZ (SPT-3G).

We simulate mm-wave data by combining the kSZ and tSZ skies from the S10 simulations with Gaussian realizations of N_ℓ, and Gaussian realizations of $C_\ell^{\rm CMB}$, the best-fit ΛCDM CMB power spectrum as constrained by SPT+WMAP in Keisler et al. (2011). We use $n_{\rm side} = 2^{13}$ Healpix[8] maps throughout our analysis.

2.3. *Signal Estimation*

Next we estimate the pairwise kSZ signal of the DES-like cluster samples in the simulated mm-wave data. One possible technique, adopted by Hand et al. (2012), is to convolve the mm-wave map with a roughly optimal spatial filter, and, for all cluster pairs $\{ij\}$ within some range of pair separation, measure

$$p_{\rm kSZ}(r) = -\frac{\Sigma_{i<j}(T_i - T_j)c_{ij}}{\Sigma_{i<j}c_{ij}^2} \quad (1)$$

where T_i is the filtered temperature at the location of cluster i, $\mathbf{r}_i$ is the comoving distance to cluster i, $\mathbf{r}_{ij} \equiv \mathbf{r}_i - \mathbf{r}_j$, and $c_{ij} \equiv \hat{\mathbf{r}}_{ij} \cdot \frac{\hat{\mathbf{r}}_i + \hat{\mathbf{r}}_j}{2}$ is a factor to account for the on-sky projection of the clusters' separation.

We instead adopt a harmonic-space technique, which we suspect may be equivalent to the real-space technique described above. We assume that, for all pairs of clusters $\{ij\}$ within a bin of cluster separation, the gravitational attraction of cluster j induces, on average, a kSZ signal at the location of cluster i given by

$$T_i(\theta) = T_0 c_{ij} \left(1 + \frac{\theta^2}{\theta_c^2}\right)^{-1} \quad (2)$$

where θ is the angle from cluster i and θ_c is the angle subtended by r_c=0.36 Mpc (physical distance). In other words, we assume a β-model profile for the optical depth to Thomson scattering with $\beta = 1$ and r_c=0.36 Mpc, which approximates the optical depth profiles of the DES-like clusters in the S10 simulations. We account for projection effects using the c_{ij} factors, which we calculate using the clusters' angular positions and simulated photometric redshifts.

Our technique boils down to fitting for T_0, the overall normalization, as a function of cluster separation and redshift. In practice this amounts to populating a blank Healpix map with the projection factors c_{ij} at the locations of all clusters in a bin of cluster separation. Specifically, we populate the position of cluster i (j) with c_{ij} (-c_{ij}), and count each pair exactly once. We convolve this map by the β-model profile to yield the kSZ template map, $\mathcal{K}$, and its spherical harmonic components $\mathcal{K}_{\ell m}$. Finally, we estimate T_0 as

$$\hat{T}_0 = \frac{\Sigma_{\ell,m}\,{\rm Re}[d_{\ell m}\mathcal{K}^*_{\ell m}]M_\ell^{-1}}{\Sigma_{\ell,m}\,{\rm Re}[\mathcal{K}_{\ell m}\mathcal{K}^*_{\ell m}]M_\ell^{-1}} \quad (3)$$

where $d_{\ell m}$ is the spherical harmonic component of a simulated mm-wave map and $M_\ell \equiv N_\ell + C_\ell^{\rm CMB}$ accounts for all sources of noise power. We repeat this procedure for several bins in pair-averaged redshift, $z_{\rm avg}$, and cluster pair separation, $r_{\rm com}$. There are three redshift bins, [{0.2, 0.4}, {0.4, 0.7}, {0.7, 1.0}], and five pair separation bins, [{10, 30}, {30, 70}, {70, 130}, {130, 200}, {200, 300}] Mpc. The kSZ signal in the bin of largest separation may be affected by the 1000 comoving Mpc/h size of the simulation box used in S10.

Many of our assumptions (*e.g.* that all clusters within a given range of redshift and cluster separation have an identical gas profile) are surely inaccurate at some level, but these assumptions can be regarded as *definitions* of the analysis technique. The technique is then calibrated by running the same analysis on simulated skies, as was done here. The challenge, of course, will be modeling

[7] https://des.fnal.gov/survey_documents/DES-DETF/Supplements_DES-DETF_v1.6.pdf

[8] http://healpix.jpl.nasa.gov

and marginalizing over the inadequacies of the simulated skies.

2.4. *Noise Estimation*

The S10 SZ maps are duplicated per octant of sky, and we assign one 2500 deg^2 SPT survey area, including unique photometric redshift errors, per octant. The CMB, instrumental noise, and point source background are generated as Gaussian realizations of M_ℓ. The kSZ amplitude T_0 is estimated once per sphere, and the scatter per survey is $\sqrt{8}$ larger than the scatter per sphere.

We simulate $\geq$120 spheres per data scenario. This ensemble of T_0 estimates is used to construct a covariance matrix C in bins of cluster separation. C is calculated per redshift bin, per data scenario.

The noise introduced by photometric redshift errors, instrumental noise, the background of point sources, and the CMB [9] are accounted for naturally in this scheme, but there is additional noise introduced by the kSZ and tSZ signals. Both of these arise from the finite number of clusters in the sample. We emphasize that the tSZ signal is not a source of bias; the pairwise kSZ signal is differential, and the tSZ will, on average, difference out.

Ideally the kSZ and tSZ noise would be estimated in the same manner as the other sources of noise — per octant, per Healpix realization — but we have only one independent octant of S10 SZ maps. Instead, we estimate the kSZ and tSZ noise using a bootstrap technique. We divide the cluster sample into eight redshift bins and measure the scatter in T_0 (at fixed cluster separation) across these redshift bins. We translate this result to our main analysis by accounting for the different redshift bin widths and by assuming that the kSZ and tSZ covariance matrices have the same dimensionless bin-bin correlation structure as the main covariance matrix C described above.

One source of noise that is absent in our analysis is velocity substructure within a cluster. S10 assigned a single peculiar velocity to all gas associated with a particular cluster when calculating the kSZ map. However, several works (*e.g.* Nagai et al. (2003), Holder (2004)) have shown that velocity substructure limits the accuracy with which mm-wave data can estimate a cluster's velocity. The systematic floor is $\sim$50-100 km/s per cluster, or $\delta T\sim2$ μK for the clusters considered here. This is completely subdominant for SPT-SZ noise levels, and unlikely to change our results for SPT-3G by more than 10%.

We have also neglected uncertainty in σ_z, the width of the photometric error distribution. The effect of photometric errors on the kSZ signal is a strong function of cluster pair separation and most strongly affects $\lesssim$50 Mpc separations, as shown in the bottom panels of Figure 1. For this reason we expect the marginalization over σ_z to only mildly weaken the utility of the pairwise kSZ measurement, especially when a prior on σ_z is provided from the broader DES analysis program.

2.5. *Results*

[9] We have neglected lensing of the CMB by the clusters, but Hezaveh et al. (2012) show that this effect only decreases the CMB variance at the cluster locations.

We use the simulations described in the previous sections to determine the detection significance of the pairwise kSZ as a function of pair-averaged redshift. Specifically, for each redshift bin we compute $\chi^2 = d^{\rm T} C d$, where d is the mean kSZ signal as a function of pair separation in this redshift bin and C is the covariance matrix described above, and calculate SNR $\equiv \sqrt{\Sigma_i \chi_i^2}$, where the sum is over the three redshift bins. We summarize the results in Table 1 and Figure 1.

We find that existing data from the SPT-SZ survey will, when combined with either of the DES samples considered here, result in a strong detection of the pairwise kSZ signal. The DES-*base* (DES-*agg*) sample yields a 8.2σ (12.9σ) detection. The smaller optical depths of the clusters in the DES-*agg* sample are made up for by the increased number density. For both samples, the measurement is largely limited by instrumental noise in the SPT-SZ data.

As expected, we find that data from a future, third-generation survey, SPT-3G, would result in even more precise measurements of the pairwise kSZ signal. The DES-*base* (DES-*agg*) sample yields a 18σ (30σ) detection. In contrast to SPT-SZ, the SPT-3G constraints are limited by kSZ and tSZ noise, with roughly equal contributions from each.

We considered using a linear combination of 95 and 150 GHz SPT-3G data to eliminate the tSZ signal and its associated variance. We found that the elimination of tSZ noise was not worth the effective increase in instrumental noise; the resulting detection significance on the DES-*agg* sample was 18σ, considerably weaker than the 30σ obtained using the original analysis.

Finally, we explored how these constraints would change in the event of spectroscopic followup of the DES cluster sample, such as would be possible with DESpec (Abdalla et al. 2012). We assume a spectroscopic redshift error of $\sigma_z = 0.002$ per cluster and find that SPT-SZ (SPT-3G) would yield a 12.5σ (26σ) detection on the DES-*base* sample and a 26σ (43σ) detection on the DES-*agg* sample.

2.6. *Implications for Testing Gravity*

The pairwise kSZ signal directly measures the average pairwise ionized momentum of a given cluster sample. The results of the previous section demonstrate that precision measurements of this signal should be available in the coming years, and these have the power to yield detailed information on the gas content of the DES clusters.

To go beyond gas physics — to constrain cosmology or gravity — we must convert to average pairwise *velocity*. This requires an independent measurement of the average ionized gas profile, say from tSZ or X-ray observations. Additionally, if there is a well motivated connection between the total cluster mass and the mass in ionized gas, then measurements of the mean mass of the sample through weak lensing or angular clustering can also constrain the conversion from kSZ signal to velocity. For the remainder of this section we assume that the uncertainty in the gas as constrained by independent data is subdominant to the uncertainty on the pairwise kSZ measurement.

The mean pairwise velocity of halos $\langle v_h \rangle(r)$ as measured through the kSZ effect as function of separation r

TABLE 1
SENSITIVITY TO PAIRWISE KSZ SIGNAL

	DES-*base* (photo-z)	DES-*agg* (photo-z)	DES-*base* (spec-z)	DES-*agg* (spec-z)
SPT-SZ	8.2σ (12%)	12.9σ (7.8%)	12.5σ (8.0%)	21σ (4.8%)
SPT-3G	18σ (5.5%)	30σ (3.3%)	26σ (3.9%)	43σ (2.3%)

The projected detection significance of the pairwise kSZ measurement for different combinations of CMB data and cluster samples.

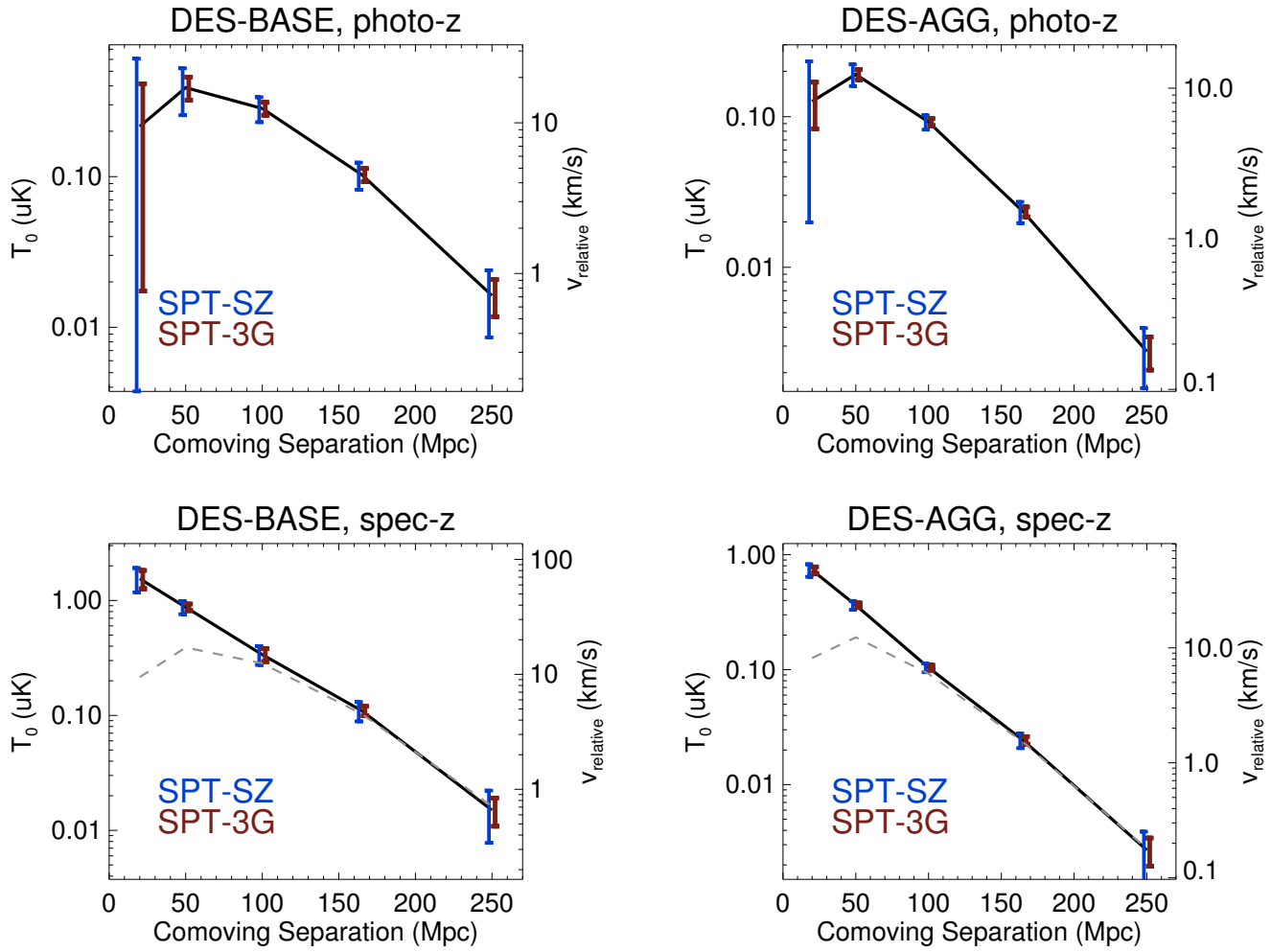

FIG. 1.— The simulated pairwise kSZ signal for the DES-*base* (*left panels*) and DES-*agg* (*right panels*) samples, and for photometric (*top panels*) and spectroscopic (*bottom panels*) redshifts. The black curve shows the mean signal, while the error bars show the projected uncertainties using data from SPT-SZ (*blue, left offset*) and SPT-3G (*red, right offset*). The *dashed, gray* curve in the bottom panels shows the mean signal using photometric redhifts, to highlight the loss of signal at $r_{\rm com} \lesssim 50$ Mpc. The errors include contributions from instrumental noise, a background of point sources, the CMB, the kSZ signal itself, and residual tSZ signal, and are mildly correlated between bins of cluster separation. The second vertical axis shows the corresponding velocity per cluster, assuming optical depths of $\tau = 0.0025$ for DES-*base* and $\tau = 0.0017$ for DES-*agg*, which are typical of the clusters used in each sample.

is in linear perturbation theory given by (Schmidt 2010)

$$\langle v_h \rangle(r) = 2\,\bar{b}\,\xi_{\delta v}(r). \quad (4)$$

Here, $\bar{b}$ is the kSZ signal-weighted mean of $(b-1)$ of halos in the given mass bin, b is the linear Eulerian bias, and $\xi_{\delta v}(r)$ is the linear cross-correlation between density and velocity. If the kSZ signal is simply proportional to gas mass which is proportional to halo mass, $\bar{b}$ reduces to the mass-weighted average of $b-1$. We assume that there is no velocity bias of halos, which holds on the large scales of interest.

The velocity-matter cross correlation is given by

$$\xi_{\delta v}(r,z) = -\frac{aHf}{2\pi^2}\int dk\, kP(k,z) j_1(kr), \quad (5)$$

where $f = d\ln D/d\ln a$ is the growth rate, $P(k,z)$ is the matter power spectrum at redshift z, and j_l denote spherical Bessel functions.

Consider a modified gravity (MG) model that leads to a scale-independent modification of growth on linear scales (one example is the Dvali-Gabadadze-Porrati (DGP) model (Dvali et al. 2000) and its generalizations). The effect of such a modification of gravity on the velocity-matter cross-correlation at fixed redshift is given by

$$\frac{\xi_{\delta v,\mathrm{MG}}(r,z)}{\xi_{\delta v,\Lambda\mathrm{CDM}}(r,z)} = \frac{[f\sigma_8^2(z)]_{\mathrm{MG}}}{[f\sigma_8^2(z)]_{\Lambda\mathrm{CDM}}}, \quad (6)$$

where $\sigma_8^2(z)$ is the power spectrum normalization at redshift z. On linear scales, the mean pairwise velocity as measured through kSZ thus constrains $\bar{b}f\,\sigma_8^2$. Independent knowledge of $\bar{b}$ can then be used to turn the kSZ measurement into a constraint on $f\sigma_8^2$. When including constraints on the expansion history and primordial amplitude of fluctuations, this can then be turned into a constraint on modified gravity. Specifically, for the normal-branch DGP model with ΛCDM expansion history considered in Schmidt (2009) which is parametrized by the cross-over scale r_c, a measurement of $\xi_{\delta v}(r)$ with an overall SNR of 10 (20) — as should be possible using the DES cluster sample in conjunction with existing data from SPT-SZ (future data from SPT-3G) — would yield a 95% confidence level lower limit of $r_c \gtrsim 3000$ (7000) Mpc, assuming that the expansion history, halo bias, and kSZ-velocity relation are known perfectly (Fig. 2). This is an interesting constraint, since a modified gravity explanation for the accelerated expansion of the Universe suggests $r_c \sim 3000h^{-1}$ Mpc as a natural value in these models.

We note that uncertainty in the cluster gas affects only the global normalization of the kSZ signal considered here, not the *shape* of the kSZ signal as a function of separation. This can be used to test the scale-dependence of gravity on sufficiently large scales, independently of gas physics. A well-studied class of modified gravity models which includes the $f(R)$ model (Carroll et al. 2004) invokes a massive additional degree of freedom. The modifications to the gravitational force and velocities are generically scale-dependent and suppressed on scales larger than the Compton length of the field, typically 30 Mpc or less (see Fig. 2). For this reason, only cluster samples with spectroscopic redshifts are useful for constraining $f(R)$. Our most optimistic scenario, in which SPT-3G observes the spectroscopically followed-up DES-*agg* cluster sample, results in a 15σ (6.7%) detection of pairwise kSZ signal in the the 10-30 Mpc separation bin. For comparison, the maximum currently-allowed value of the field amplitude in the Hu & Sawicki (2007) $f(R)$ model is $|f_{R0}| = 10^{-4}$ (Schmidt et al. 2009; Lombriser et al. 2012), and results in a ∼25% increase in $\xi_{\delta v}$ over this range. The SPT-3G+DES-*agg*(spec-z) scenario would therefore allow a 4σ test of this hypothesis.

3. DISCUSSION

We have estimated the sensitivity of mm-wave data from SPT to the pairwise kSZ signal of clusters from the DES. We find that existing SPT data will allow for an 8-13σ detection of the kSZ signal. If the kSZ-velocity relation is known perfectly, this corresponds to an 8-12% constraint on $f\sigma_8^2$, which is comparable to the current best constraint on growth from redshift space distortions (RSD), an 8.2% constraint on $f\sigma_8$ from BOSS (Reid et al. 2012).

The difference is that the bulk of the RSD sensitivity arises from quasi-linear scales (Reid & White 2011), whereas the SPT+DES kSZ signal is most sensitive to significantly larger, more easily modeled, linear scales. This is due to the DES photometric redshifts, and spectroscopic followup would boost the kSZ SNR by a factor of 1.5. A third-generation SPT survey would improve any of these constraints by a factor of ∼2.1, and is limited largely by noise from the kSZ and tSZ signals. These measurements have the potential to provide interesting constraints on theories of modified gravity.

We thank Lloyd Knox, Gil Holder, Tom Crawford, Eduardo Rozo, and Christian Reichardt for useful conversations regarding this work, and the Texas Cosmology Center at the University of Texas at Austin — where this work was initiated — for its hospitality. RK acknowledges support from NASA Hubble Fellowship grant HF-51275, and FS from the NASA Einstein Fellowship. This research used resources from the RCC at the University of Chicago and NERSC, which is supported by the U.S. DOE under Contract DE-AC02-05CH11231

REFERENCES

Abdalla, F., et al. 2012, ArXiv e-prints, 1209.2451
Benson, B. A., et al. 2011, arXiv:1112.5435
Bhattacharya, S., & Kosowsky, A. 2007, ApJ, 659, L83
Carlstrom, J. E., et al. 2011, PASP, 123, 568
Carroll, S. M., Duvvuri, V., Trodden, M., & Turner, M. S. 2004, Phys. Rev., D70, 043528
Dvali, G., Gabadadze, G., & Porrati, M. 2000, Physics Letters B, 485, 208
Hand, N., et al. 2012, arXiv:1203.4219
Hezaveh, Y., Vanderlinde, K., Holder, G., & de Haan, T. 2012, ArXiv e-prints, 1210.6354
Holder, G. P. 2004, ApJ, 602, 18
Hu, W., & Sawicki, I. 2007, Phys. Rev. D, 76, 064004
Keisler, R., et al. 2011, ApJ, 743, 28
Kosowsky, A., & Bhattacharya, S. 2009, Phys. Rev. D, 80, 062003
Lombriser, L., Slosar, A., Seljak, U., & Hu, W. 2012, Phys. Rev. D, 85, 124038
Nagai, D., Kravtsov, A. V., & Kosowsky, A. 2003, ApJ, 587, 524

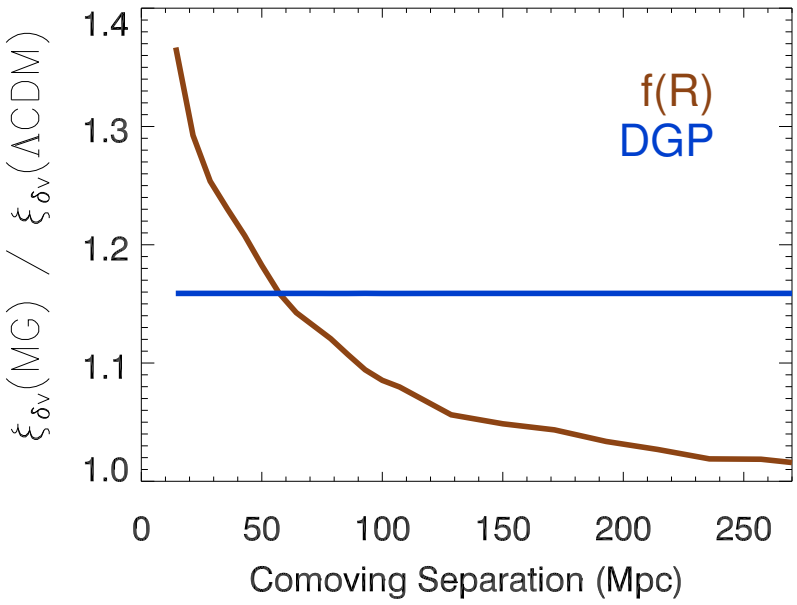

FIG. 2.— The change in the density-velocity correlation function $\xi_{\delta v}$ in two models of modified gravity. The $f(R)$ model uses $|f_{R0}| = 10^{-4}$, the maximum field value currently allowed. The DGP model uses $r_c = 4000$ Mpc.

Reichardt, C. L., et al. 2012, ApJ, 755, 70
Reid, B. A., et al. 2012, MNRAS, 426, 2719
Reid, B. A., & White, M. 2011, MNRAS, 417, 1913
Reyes, R., Mandelbaum, R., Seljak, U., Baldauf, T., Gunn, J. E., Lombriser, L., & Smith, R. E. 2010, Nature, 464, 256
Ross, A. J., Percival, W. J., Crocce, M., Cabré, A., & Gaztañaga, E. 2011, MNRAS, 415, 2193
Rykoff, E. S., et al. 2012, ApJ, 746, 178
Schmidt, F. 2009, Phys. Rev. D, 80, 123003
——. 2010, Phys. Rev. D, 82, 063001
Schmidt, F., Vikhlinin, A., & Hu, W. 2009, Phys. Rev., D80, 083505
SDSS-III Collaboration, et al. 2012, ArXiv e-prints, 1207.7137
Sehgal, N., Bode, P., Das, S., Hernandez-Monteagudo, C., Huffenberger, K., Lin, Y., Ostriker, J. P., & Trac, H. 2010, ApJ, 709, 920
Sunyaev, R. A., & Zel'dovich, Y. B. 1972, Comments on Astrophysics and Space Physics, 4, 173